International Journal of Thermophysics, Vol. 23, No. 6, November 2002 (© 2002)

The Dual-Phase-Lag Heat Conduction Model in Thin Slabs Under a Fluctuating Volumetric Thermal Disturbance

M. A. Hader,[1] **M. A. Al-Nimr,**[1, 2] **and B. A. Abu Nabah**[3]

Received December 12, 2001

In the present work, the thermal behavior of a thin slab, under the effect of a fluctuating volumetric thermal disturbance described by the dual-phase-lag heat conduction model is investigated. It is found that the use of the dual-phase-lag heat conduction model is essential at large frequencies of the volumetric disturbance. It is found that the hyperbolic wave model deviates from the diffusion model when $\bar{\omega} > \frac{0.01}{\bar{\tau}_q}$ and the dual-phase-lag model deviates from the diffusion model when $\bar{\omega} > \frac{0.01}{\bar{\tau}_T}$. where $\bar{\omega}$ is the angular velocity of the fluctuating wall temperature, $\bar{\tau}_q$ is the phase-lag in the heat flux vector and $\bar{\tau}_T$ is the phase-lag in the temperature gradient vector.

KEY WORDS: dual-phase-lag model; heat conduction; fluctuating thermal disturbance.

1. INTRODUCTION

For situations involving very low temperatures near absolute zero, for a heat source such as a laser or microwave of extremely short duration or very high frequency, very high temperature gradient and extremely short times, heat is found to propagate at a finite speed. To account for the phenomena involving the finite propagation velocity of the thermal wave, the classical Fourier heat flux model should be modified. Cattaneo [1] and

[1] Mechanical Engineering Department, Jordan University of Science and Technology, Irbid 22110, Jordan.
[2] To whome correspondence should be addressed. E-mail: malnimr@just.edu.jo
[3] Department of Mechanical Engineering, University of Cincinnati, Cincinnati, Ohio 45221, U.S.A.

0195-928X/02/1100-1669/0 © 2002 Plenum Publishing Corporation

Vernotte [2] suggested independently a modified heat flux model in the form of

$$\vec{q}(t+\bar{\tau}_q, \vec{r}) = -k\,\vec{\nabla}T(t, \vec{r}) \tag{1}$$

where $\vec{q}$ is the heat flux vector, k is the thermal conductivity and $\bar{\tau}_q$ is the phase-lag in the heat flux vector. The constitutive law of Eq. (1) assumes that the heat flux vector (the effect) and the temperature gradient (the cause) across a material volume occur at different instants of time and the time delay between the heat flux and the temperature gradient is the relaxation time $\bar{\tau}_q$. The first-order expansion of $\vec{q}$ in Eq. (1) with respect to t bridges all the physical quantities at the same time. It results in the expansion:

$$\vec{q}(t, \vec{r}) + \bar{\tau}_q \frac{\partial \vec{q}}{\partial t}(t, \vec{r}) = -k\,\vec{\nabla}T(t, \vec{r}) \tag{2}$$

In Eq. (2) it is assumed that $\bar{\tau}_q$ is sufficiently small such that the first-order Taylor expansion of $\vec{q}(t+\bar{\tau}_q, \vec{r})$ is an accurate representation for the conduction heat flux vector. The equation of energy conservation for such problems is given as

$$\rho c \frac{\partial T}{\partial t} = -\vec{\nabla} \cdot \vec{q} + g \tag{3}$$

where ρ is the density, g is heat generation per unit volume, and c is the specific heat. Elimination of $\vec{q}$ between Eqs. (2) and (3) leads to the classical hyperbolic heat conduction equation:

$$\frac{1}{\alpha}\frac{\partial T}{\partial t} + \frac{\bar{\tau}_q}{\alpha}\frac{\partial^2 T}{\partial t^2} = \nabla^2 T + \frac{g}{k} + \frac{\bar{\tau}_q}{k}\frac{\partial g}{\partial t} \tag{4}$$

To remove the causality assumption made in the thermal wave model, as proposed in Eq. (1), the dual-phase-lag model is proposed [3–5]. The dual-phase-lag model allows either the temperature gradient (cause) to precede the heat flux vector (effect) or the heat flux vector (cause) to precede the temperature gradient (effect) in the transient process. Mathematically, this can be represented by [3–5]:

$$\vec{q}(t+\bar{\tau}_q, \vec{r}) = -k\,\vec{\nabla}T(t+\bar{\tau}_T, \vec{r}) \tag{5}$$

where $\bar{\tau}_T$ is the phase-lag in the temperature gradient vector and $\bar{\tau}_q$ is the phase-lag in the heat flux vector. For the case of $\bar{\tau}_T > \bar{\tau}_q$, the temperature gradient established across a material volume is a result of the heat flow, implying that the heat flux vector is the cause and the temperature gradient is the effect. For $\bar{\tau}_T < \bar{\tau}_q$, on the other hand, heat flow is induced by the temperature gradient established at an earlier time, implying that the temperature gradient is the cause, while the heat flux vector is the effect. The first-order approximation of Eq. (5) yields

$$\vec{q}(t,\vec{r})+\bar{\tau}_q \frac{\partial \vec{q}}{\partial t}(t,\vec{r}) = -k\left\{\vec{\nabla}T(t,\vec{r})+\bar{\tau}_T \frac{\partial}{\partial t}[\vec{\nabla}T(t,\vec{r})]\right\} \tag{6}$$

Elimination of $\vec{q}$ between Eqs. (3) and (6) leads to the heat conduction equation under the dual-phase-lag effect:

$$\frac{1}{\alpha}\frac{\partial T}{\partial t}(t,\vec{r})+\frac{\bar{\tau}_q}{\alpha}\frac{\partial^2 T}{\partial t^2}(t,\vec{r}) = \nabla^2 T(t,\vec{r})+\bar{\tau}_T \frac{\partial}{\partial t}[\nabla^2 T(t,\vec{r})]+\frac{1}{k}\left[g+\bar{\tau}_q \frac{\partial g}{\partial t}(t,\vec{r})\right] \tag{7}$$

In the absence of the temperature gradient phase-lag ($\bar{\tau}_T = 0$), Eq. (7) reduces to the classical hyperbolic heat conduction equation as described by Eq. (4). Also, in the absence of the two phase-lags ($\bar{\tau}_T = \bar{\tau}_q = 0$), Eq. (7) reduces to the classical diffusion equation employing Fourier's law.

In the literature, numerous studies [6–13] have been conducted to investigate the thermal behavior of slabs subject to non-fluctuating heating sources under the effect of the hyperbolic and the dual-phase-lag heat conduction models . On the other hand, very few studies [14–16] have been conducted to investigate the thermal behavior of domains subject to harmonic fluctuating thermal disturbances under the effect of the hyperbolic heat conduction model. Based on the authors' knowledge, the thermal behavior of these systems under the effect of the dual-phase-lag heat conduction model has not yet been investigated. In the present work, the thermal behavior of thin layers subject to fluctuating volumetric thermal disturbances under the effect of the dual-phase-lag heat conduction model will be investigated. The role that the frequency of the fluctuating volumetric disturbance plays in using the appropriate heat conduction model will be studied.

2. ANALYSIS

Consider a thin layer of thickness 2L for which the boundaries are maintained at a fixed temperature T_w and within which a volumetric heating source g fluctuates in a harmonic manner. Using the dimensionless parameters defined in the nomenclature, the governing equations are expressed as

$$\frac{\partial \theta}{\partial \eta}+\tau_q \frac{\partial^2 \theta}{\partial \eta^2}=\frac{\partial^2 \theta}{\partial \xi^2}+\tau_T \frac{\partial^3 \theta}{\partial \eta \partial \xi^2}+G+\tau_q \frac{\partial G}{\partial \eta} \tag{8}$$

$$\frac{\partial \theta}{\partial \xi}(\eta, 0)=0, \qquad \theta(\eta, 1)=0. \tag{9}$$

Now, assuming the volumetric heating source G to fluctuate in the following harmonic manner,

$$G=1+\epsilon \sin(\omega\eta)=1+\epsilon \Im\{e^{i\omega\eta}\} \tag{10}$$

As a result, Eq. (8) may be written as

$$\frac{\partial \theta}{\partial \eta}+\tau_q \frac{\partial^2 \theta}{\partial \eta^2}=\frac{\partial^2 \theta}{\partial \xi^2}+\tau_T \frac{\partial^3 \theta}{\partial \eta \partial \xi^2}+1+\epsilon \Im\{e^{i\omega\eta}\}+\tau_q \epsilon \omega i \Im\{e^{i\omega\eta}\} \tag{11}$$

where $\Im$ represents the “imaginary part of” and the origin of the ξ-axis is located at the plate center line.

Equations (11) and (9) assume a solution in the form:

$$\theta(\eta, \xi)=\theta_s(\xi)+\theta_u(\eta, \xi) \tag{12}$$

where $\theta_s(\xi)$ and $\theta_u(\eta, \xi)$ satisfy the following governing equations:

$$\frac{\partial^2 \theta_s}{\partial \xi^2}+1=0 \tag{13}$$

$$\frac{\partial \theta_s}{\partial \xi}(\eta, 0)=0, \qquad \theta_s(\eta, 1)=0 \tag{14}$$

$$\frac{\partial \theta_u}{\partial \eta}+\tau_q \frac{\partial^2 \theta_u}{\partial \eta^2}=\frac{\partial^2 \theta_u}{\partial \xi^2}+\tau_T \frac{\partial^3 \theta_u}{\partial \eta \partial \xi^2}+\epsilon \Im\{e^{i\omega\eta}\}+\tau_q \epsilon \omega i \Im\{e^{i\omega\eta}\} \tag{15}$$

$$\frac{\partial \theta_u}{\partial \xi}(\eta, 0)=0, \qquad \theta_u(\eta, 1)=0 \tag{16}$$

Equations (13) and (14) assume a solution in the form:

$$\theta_s(\xi)=\tfrac{1}{2}(1-\xi^2) \tag{17}$$

while Eqs. (15) and (16) assume a solution in the form

$$\theta_u(\eta, \xi) = \Im\{W(\xi)\, e^{i\omega\eta}\} \tag{18}$$

Inserting Eq. (18) into Eqs. (15) and (16) yields

$$\frac{d^2W}{d\xi^2} - \lambda^2 W = -\beta \tag{19}$$

$$\frac{dW}{d\xi}(0) = 0, \qquad W(1) = \epsilon \tag{20}$$

where

$$\lambda^2 = \frac{\omega i - \tau_q \omega^2}{1 + \tau_T \omega i} \quad \text{and} \quad \beta = \frac{\epsilon(1 + \tau_q \omega i)}{1 + \tau_T \omega i} \tag{21}$$

Equations (19) and (20) have the following solution:

$$W(\xi) = \frac{\beta}{\lambda^2}\left[1 - \frac{\cosh(\lambda\xi)}{\cosh(\lambda)}\right] \tag{22}$$

As a result, the governing Eqs. (8)–(10) assume the following solution,

$$\theta(\eta, \xi) = \frac{1}{2}(1 - \xi^2) + \Im\left\{e^{i\omega\eta}\frac{\beta}{\lambda^2}\left[1 - \frac{\cosh(\lambda\xi)}{\cosh(\lambda)}\right]\right\} \tag{23}$$

In the following section, results are obtained for three models, which are the dual-phase-lag model, the hyperbolic model ($\tau_T = 0$), and the diffusion model ($\tau_T = \tau_q = 0$).

3. RESULTS AND DISCUSION

The parameter λ^2 in Eq. (21) is normalized in the following manner,

$$\frac{\lambda^2}{\omega} = \frac{i - \tau_q \omega}{1 + \tau_T \omega i} \tag{24}$$

For the parabolic heat conduction model with $\tau_T = \tau_q = 0$, Eq. (24) becomes

$$\frac{\lambda^2}{\omega} = i \tag{25}$$

and for the hyperbolic heat conduction model with $\tau_T = 0$, Eq. (24) becomes

$$\frac{\lambda^2}{\omega} = -\omega\tau_q + i \tag{26}$$

Also, the parameter $\frac{\beta}{\lambda^2}$ appearing in the solution, Eq. (22), is normalized in the following manner,

$$\frac{\beta\omega}{\lambda^2} = \frac{\epsilon(1+\tau_q\omega i)}{i-\tau_q\omega} \tag{27}$$

Equation (27) is also valid for the hyperbolic heat conduction model. For the parabolic model, Eq. (27) reduces to

$$\frac{\beta\omega}{\lambda^2} = -\epsilon i \tag{28}$$

Now, with the notation that

$$\frac{1}{1+\tau_T\omega i} \approx 1-\tau_T\omega i, \qquad \omega\tau_T \ll 1,$$

Eq. (24) may be approximated as

$$\frac{\lambda^2}{\omega} = i(1+\tau_q\tau_T\omega^2) + (\tau_T-\tau_q)\,\omega i \tag{29}$$

A comparison between Eqs. (25) and (26) reveals that the predictions of the hyperbolic wave model deviate from those of the parabolic model, by more than 1% in the normalized quantity $\frac{\lambda^2}{\omega}$, when

$$\bar{\omega} > \frac{0.01}{\bar{\tau}_q} \tag{30}$$

On the other hand, a comparison between Eqs. (25) and (29) reveals that the predictions of the dual-phase-lag model deviate from those of the parabolic model, by more than 1% in the normalized quantity $\frac{\lambda^2}{\omega}$, when

$$\bar{\omega} > \frac{0.01}{\bar{\tau}_T}, \qquad \bar{\omega} > \frac{0.1}{\sqrt{\bar{\tau}_T\bar{\tau}_q}} \tag{31}$$

Taking into consideration that for most metals $\bar{\tau}_T \sim 100\bar{\tau}_q$, it may be concluded that the first criterion in Eq. (31) is the dominant one.

In a similar manner, the parameter $\frac{\beta\omega}{\lambda^2}$ may be approximated as

$$\frac{\beta\omega}{\lambda^2} = -\epsilon(1+\tau_q^2\omega^2)\, i \tag{32}$$

A comparison between Eqs. (28) and (32) reveals that the predictions of both the dual-phase-lag and hyperbolic models deviate from those of the parabolic model, by more than 1% in the normalized quantity $\frac{\beta\omega}{\lambda^2}$, when

$$\bar{\varpi} > \frac{0.1}{\bar{\tau}_q} \tag{33}$$

From the three criteria which account for the deviations of the dual-phase-lag model from the parabolic model, it is clear that the first criterion in Eq. (31) is the dominant one. On the other hand, the criterion, Eq. (30), is the dominant criterion for the deviations between the hyperbolic and the parabolic models. For most pure metals, $\bar{\tau}_q \sim 1 \times 10^{-12} s$ and $\bar{\tau}_T \sim 1 \times 10^{-10} s$, and the criterion in Eq. (30) reveals that using the hyperbolic model is essential when $\bar{\varpi} > 1 \times 10^{10}$ rad $\cdot$ s^{-1}. On the other hand, the first criterion in Eq. (31) reveals that using the dual-phase-lag model is essential when $\bar{\varpi} > 1 \times 10^{8}$ rad $\cdot$ s^{-1}. This is an important conclusion which reveals that the dual-phase-lag model starts to deviate from the diffusion model before the hyperbolic model. However, the hyperbolic model is used more frequently because of its simplicity.

Figure 1 shows the harmonic variations in temperature as predicted by the three models at different dimensionless angular velocities ω. It is clear from this figure that the deviation between the dual-phase-lag model and the parabolic model appears at dimensionless frequencies ω higher than 0.1. Most metal slabs have $\alpha \sim 10^{-4}$ m$^2 \cdot$ s^{-1} and thickness $L = 10^{-7}$ m, which is the typical thickness in which the non-Fourier heat conduction models find applications, and as a result, the deviation from the parabolic model appears when $\bar{\varpi} > 10^9$ rad $\cdot$ s^{-1}, where $\bar{\varpi} = \frac{\alpha\omega}{L^2}$. This agrees very well with the predictions of the first criterion in Eq. (31). Figure 1 shows that the deviation of the dual-phase-lag model from the parabolic model appears at lower frequencies as compared to the deviation of the hyperbolic model from the parabolic model. As clear from Fig. 1, the hyperbolic model starts to deviate from the parabolic one at dimensionless frequencies higher than 1 which correspond to $\bar{\varpi} > 10^{10}$ rad $\cdot$ s^{-1}. Also, this agrees very well with the previous conclusions obtained from the criterion of Eq. (30). However, it should be noted that such high frequencies are unattainable

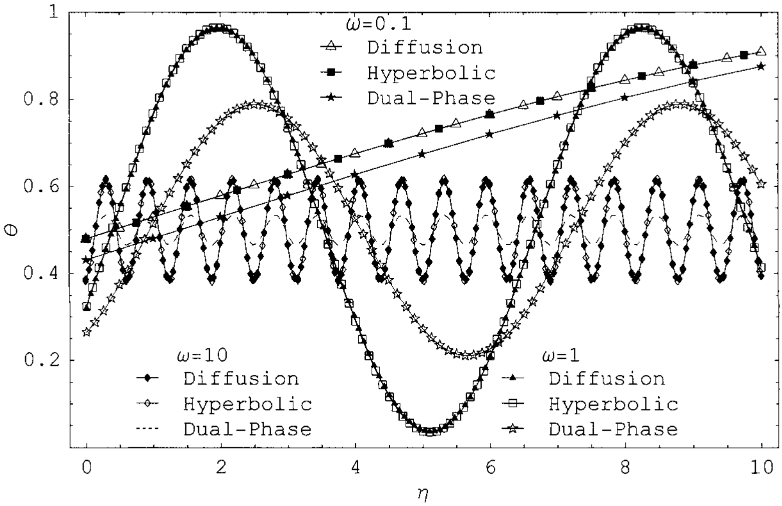

Fig. 1. Harmonic variation in the slab temperature as predicted by the three models. ($\xi = 0.0$, $\tau_q = 0.01$, $\tau_T = 1.0$, $\epsilon = 1.0$).

experimentally. The temperature amplitude versus angular frequency for the three models is shown in Fig. 2. It is clear from Fig. 2 that as the angular frequency increases, the intensity of the thermal response decreases. This is due to the fact that the total heat absorbed by the slab from the heating source is proportional to $\frac{1}{\omega}$. It is clear from this figure that the

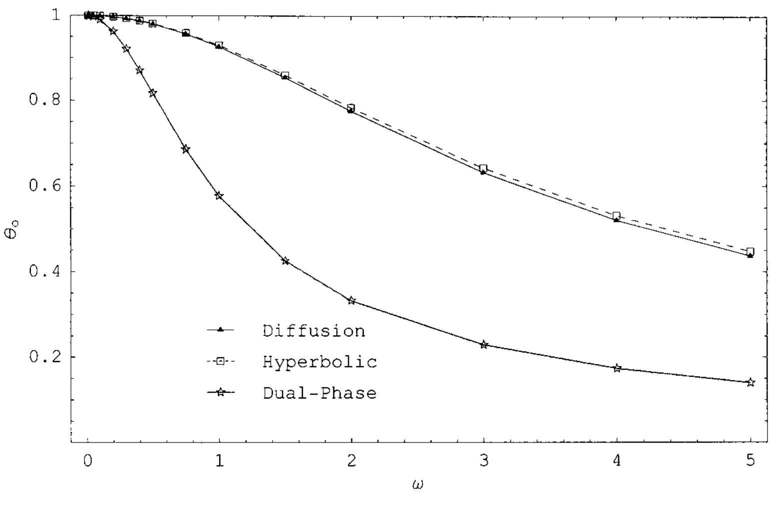

Fig. 2. Temperature amplitude versus angular frequency in the slab as predicted by the three models ($\tau_q = 0.01$, $\tau_T = 1.0$, $\epsilon = 1.0$).

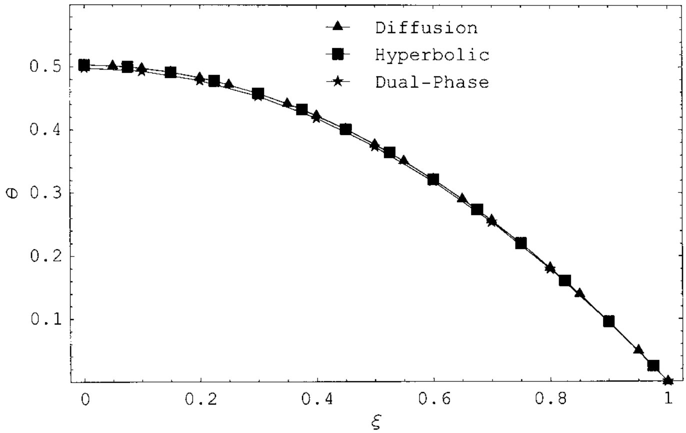

Fig. 3. Temperature spatial distribution within the slab as predicted by the three models ($\omega = .01$, $\eta = 1.0$, $\tau_q = 0.01$, $\tau_T = 1.0$, $\epsilon = 1.0$).

deviation between the hyperbolic and the diffusion models is insignificant especially at small ω, while the deviation of the dual-phase-lag model from the other two models is significant over a wider frequency ranges. The phase lag increases as ω increases. However, this increse saturates as ω increases and reach an asymptotic value.

The spatial distribution of the temperature at different frequencies and for the three models is shown in Figs. 3 to 5. It is clear from these figures that the deviation between the dual-phase-lag model and both the parabolic and hyperbolic models is larger far from the slab boundary. The

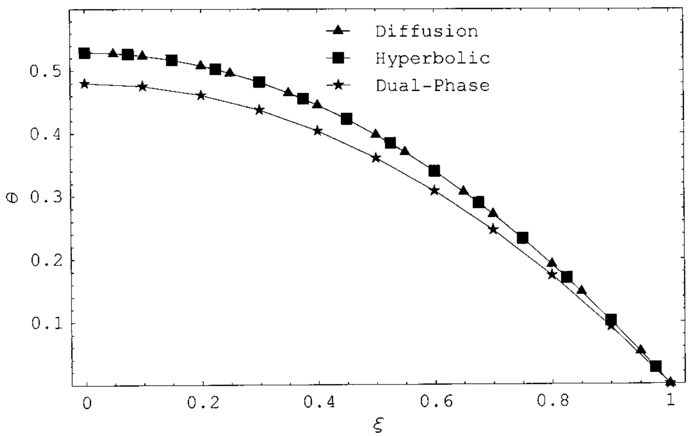

Fig. 4. Temperature spatial distribution within the slab as predicted by the three models ($\omega = 0.1$, $\eta = 1.0$, $\tau_q = 0.01$, $\tau_T = 1.0$, $\epsilon = 1.0$).

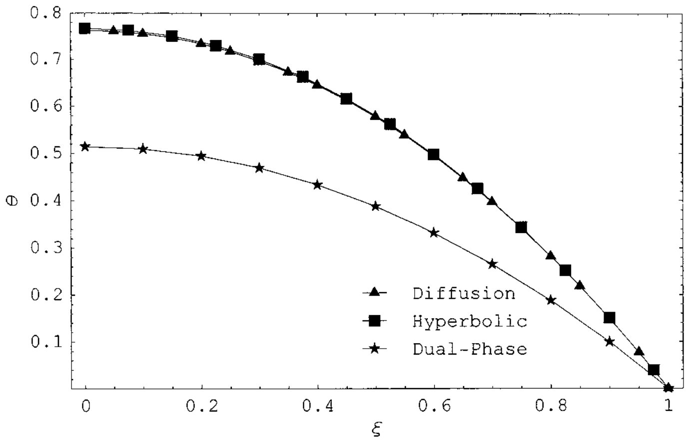

Fig. 5. Temperature spatial distribution within the slab as predicted by the three models ($\omega = 1.0$, $\eta = 1.0$, $\tau_q = 0.01$, $\tau_T = 1.0$, $\epsilon = 1.0$).

cooling effect at the slab boundary reduces the differences in temperature among the predictions of the three models at these locations.

4. CONCLUSION

The deviations among three macroscopic heat conduction models under the effect of a fluctuating volumetric heating source, which heats a thin layer, are investigated. These three models are the parabolic, hyperbolic, and dual-phase-lag heat conduction models. The heating disturbance is assumed to fluctuate in a harmonic manner. It is found that using the dual-phase-lag heat conduction model is essential at large frequencies of the surface disturbance. It is found that the hyperbolic wave model deviates from the diffusion model when $\bar{\omega} > \frac{0.01}{\bar{\tau}_q}$ and the dual-phase-lag model deviates from the diffusion model when $\bar{\omega} > \frac{0.01}{\bar{\tau}_T}$. The dual-phase-lag model starts to deviate from the parabolic model at lower frequencies as compared to deviations of the hyperbolic model from the parabolic model. The phase-shift between each two of the three models increases as the frequency increases but it reaches an asymptote at very high frequencies.

NOMENCLATURE

c specific heat capacity
g heating source per unit volume, $g_o(1+\epsilon \sin(\bar{\omega}t))$

g_o amplitude of the heating source
G dimensionless volumetric heating source, $\frac{g}{g_o}$
i imaginary number, $\sqrt{-1}$
k thermal conductivity
2L slab thickness
q conduction heat flux
t time
T temperature
T_w wall temperature
W temperature spatial amplitude
x axial coordinate

GREEK SYMBOLS

α thermal diffusivity, $\frac{k}{\rho c}$
ϵ amplitude of fluctuation in heating source
η dimensionless time, $\frac{\alpha t}{L^2}$
ρ density
θ dimensionless temperature, $\frac{k(T-T_w)}{L^2 g_o}$
θ_o amplitude of dimensionless temperature, $\frac{k(T_o-T_w)}{L^2 g_o}$
$\bar{\tau}_q$ phase-lag in heat flux
τ_q dimensionless phase-lag in heat flux, $\frac{\alpha\bar{\tau}_q}{L^2}$
$\bar{\tau}_T$ phase-lag in temperature gradient
τ_T dimensionless phase-lag in temperature gradient, $\frac{\alpha\bar{\tau}_T}{L^2}$
ξ dimensionless axial coordinate, $\frac{x}{L}$
$\bar{\omega}$ angular velocity of the fluctuating wall temperature
ω dimensionless angular velocity of the fluctuating wall temperature, $\frac{\bar{\omega}L^2}{\alpha}$

REFERENCES

1. C. Cattaneo, *Comptes Rendus* **247**:431 (1958).
2. P. Vernotte, *Comptes Rendus* **252**:2190 (1961).
3. D. Y. Tzou, *ASME J. Heat Transfer* **117**:8 (1995).
4. D. Y. Tzou, *Int. J. Heat and Mass Transfer* **38**:3231 (1995).
5. D. Y. Tzou, *AIAA J. Thermophys. Heat Transfer* **9**:686 (1995).
6. W. S. Kim, L. G. Hector, and M. N. Ozisik, *J. Applied Phys.* **68**:5478 (1990).
7. M. N. Ozisik and D. Y. Tzou, *ASME J. Heat Transfer* **116**:526 (1994).
8. M. A. Al-Nimr and M. Naji, *Int. J. Thermophys.* **21**:281 (2000).
9. M. A. Al-Nimr and M. Naji, *Microscale Thermophys. Eng.* **4**:231 (2000).
10. M. A. Al-Nimr, M. Naji, and V. Arpaci, *ASME J. Heat Transfer* **122**:217 (2000).

11. M. A. Al-Nimr and N. Al-Huniti, *J. Thermal Stresses* **23**:731 (2000).
12. M. A. Al-Nimr and M. A. Hader, *Heat Transfer Eng*. **22**:1 (2001).
13. M. A. Al-Nimr and O. M. Haddad, *Heat Mass Transfer*. **37**:175 (2001).
14. D. W. Tang and N. Araki, *Int. J. Heat Mass Transfer*. **39**:1585 (1996).
15. J. Golebiowski and A. J. Jordan, *Int. J. Heat Mass Transfer*. **36**:3099 (1993).
16. W. Yuen and S. Lee, *ASME J. Heat Transfer* **111**:178 (1989).